Electronic Supplementary Material (ESI) for Physical Chemistry Chemical Physics.

english

A Force Field for Bio-Polymers in Ionic Liquids (BILFF) – Part 2: Cellulose in [EMIm][OAc] / Water Mixtures

Supporting Information

Eliane Roos, Daniel Sebastiani and Martin Brehm*

Institut für Chemie - Theoretische Chemie, Martin-Luther-Universität Halle-Wittenberg, Von-Danckelmann-Platz 4, 06120 Halle (Saale), Germany.

*E-mail: Martin_Brehm@gmx.de

*Website: https://brehm-research.de/

1 Force Field Parameters

In this section, our optimized force field parameters for cellulose in pure and aqueous [EMIm][OAc] are presented. The nomenclature used for the atom types *(used for the non-bonded interactions)* can be found in Figure S–1 while the atom classes *(used for the bonded interactions)* are shown in Table S–1. Please note that the atom types OH1, HO1, OH4, and HO4 correspond to terminal hydroxyl groups and are found only once on each end of the cellulose strand. The force field is based on the potential energy equation of the OPLS–AA force field: [1–3]

$$\begin{aligned} U(r^N) = & \sum_{i \in \text{bonds}} k_{l,i}(l_i - l_{i,0})^2 + \sum_{i \in \text{angles}} k_{\theta,i}(\theta_i - \theta_{i,0})^2 \\ & + \sum_{i \in \text{dihedrals}} \left[\frac{V_{i,1}}{2}[1 + \cos(\phi_\text{i})] + \frac{V_{i,2}}{2}[1 - \cos(2\phi_\text{i})] \right. \\ & \qquad \left. + \frac{V_{i,3}}{2}[1 + \cos(3\phi_\text{i})] + \frac{V_{i,4}}{2}[1 - \cos(4\phi_\text{i})] \right] \\ & + \sum_{i=1}^{N} \sum_{j=i+1}^{N} \left[4\epsilon_{ij} \left[\left(\frac{\sigma_{ij}}{r_{ij}} \right)^{12} - \left(\frac{\sigma_{ij}}{r_{ij}} \right)^{6} \right] + \frac{q_i q_j e^2}{4\pi\epsilon_0 r_{ij}} \right] f_{ij} \,. \end{aligned} \tag{S–1}$$

$$\epsilon_{i,j} = \sqrt{\epsilon_i \, \epsilon_j}, \qquad \sigma_{i,j} = \sqrt{\sigma_i \, \sigma_j} \tag{S–2}$$

The force constants k for the bonds and angles and the torsion parameters V in Tab. S–2, S–3, S–4, and S–5 do not include the factor 1/2. In accordance with OPLS–AA, the interactions between the atomic neighbors 1–2 and 1–3 were not taken into account; the 1–4 interactions were scaled with $f_{ij} = 0.5$. For the Lennard-Jones cross terms, geometric mixing rules were applied *(see Equation S–2)*. The Coulomb and Lennard-Jones cutoff radius were set to 800 pm. For the Coulomb interactions, the PPPM long-range Coulomb solver (as implemented in LAMMPS) [4] was applied. For [EMIm][OAc], the force field BILFF [5] and for water TIP4P–EW [6] (with constrained bonds and angles) was used without modifications. The total charge of the ions amounts to ±0.82 in BILFF. [5]

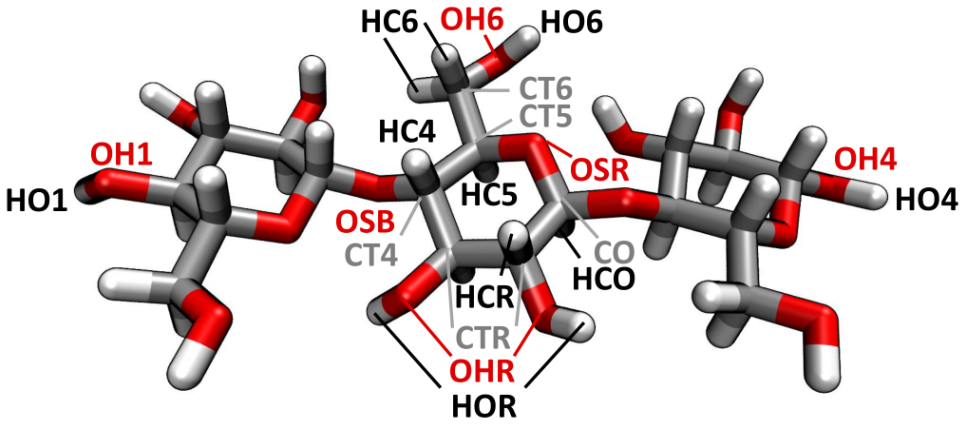

Figure S–1: Nomenclature of cellulose atom types in our force field BILFF. The corresponding atom classes are listed in Table S–1.

Table S–1: Nomenclature of atom types and atom classes in cellulose. The atom types are used for the non-bonded interactions *(see Table S–2)*, while the atom classes are used for the bonded interactions *(see Tables S–3*, S–4, and S–5).

Atom Type	Atom Class
CO	CO
CTR	CT
CT4	CT
CT5	CT
CT6	CT
OSB	OSB
OSR	OSR
OH1	OH
OH4	OH
OHR	OH
OH6	OH
HCO	HC
HCR	HC
HC4	HC
HC5	HC
HC6	HC
HOR	HO
HO1	HO
HO4	HO
HO6	HO

Table S–2: Optimized atomic partial charges q and Lennard-Jones parameters σ and ϵ for cellulose in comparison to the literature force field of W. Damm *et al.*[7]

Atom Type	BILFF			Literature[7]		
	q	σ / Å	ϵ / kJ mol^{-1}	q	σ / Å	ϵ / kJ mol^{-1}
CO	0.3050	3.50	0.27614	0.3000	3.50	0.27614
CTR	0.2100	3.50	0.27614	0.2050	3.50	0.27614
CT4	0.2100	3.50	0.27614	0.2050	3.50	0.27614
CT5	0.1750	3.50	0.27614	0.1700	3.50	0.27614
CT6	0.1600	3.50	0.27614	0.1450	3.50	0.27614
OSB	−0.3890	2.90	0.58576	−0.3970	2.90	0.58576
OSR	−0.3887	2.90	0.58576	−0.4000	2.90	0.58576
OH1	−0.6920	3.07	0.71128	−0.7000	3.07	0.71128
OH4	−0.6180	3.07	0.71128	−0.7000	3.07	0.71128
OHR	−0.6850	3.07	0.71128	−0.7000	3.07	0.71128
OH6	−0.6600	3.12	0.71128	−0.6830	3.12	0.71128
HCO	0.1060	2.60	0.12552	0.1000	2.50	0.12552
HCR	0.0450	2.60	0.12552	0.0600	2.50	0.12552
HC4	0.0460	2.60	0.12552	0.0600	2.50	0.12552
HC5	0.0370	2.60	0.12552	0.0300	2.50	0.12552
HC6	0.0470	2.60	0.12552	0.0600	2.50	0.12552
HOR	0.3790	1.00	0.12552	0.4350	0.00	0.00000
HO1	0.4280	1.00	0.12552	0.4350	0.00	0.00000
HO4	0.4930	1.10	0.12552	0.4350	0.00	0.00000
HO6	0.4067	0.97	0.12552	0.4180	0.00	0.00000

Table S–3: Optimized bond equilibrium lengths l_0 and force constants k_l for cellulose in comparison to the literature force field of W. Damm *et al.*[7]

Bond	BILFF		Literature[7]	
	l_0 / Å	k_l / kJ mol^{-1} Å^{-2}	l_0 / Å	k_l / kJ mol^{-1} Å^{-2}
CT–OSB	1.446	1815.7	1.410	1338.9
CT–OSR	1.442	1867.2	1.410	1338.9
CT–OH	1.440	2138.9	1.410	1338.9
CO–OSB	1.405	2001.7	1.380	1338.9
CO–OSR	1.441	1610.2	1.380	1338.9
CO–OH	1.441	2288.5	1.380	1338.9
CT–CT	1.530	1789.1	1.529	1121.3
CT–CO	1.527	1819.3	1.529	1121.3
CT–HC	1.101	2801.1	1.090	1422.6
CO–HC	1.101	2880.5	1.090	1422.6
OH–HO	0.965	3054.5	0.945	2313.8

Table S–4: Optimized angle equilibrium values θ_0 and force constants k_θ for cellulose in comparison to the literature force field of W. Damm *et al.*[7]

Angle	BILFF		Literature[7]	
	θ_0 / Deg	k_θ / kJ mol^{-1} rad^{-2}	θ_0 / Deg	k_θ / kJ mol^{-1} rad^{-2}
CT–CT–CT	113.64	458.5	112.7	244.1
CT–CT–CO	112.38	407.4	112.7	244.1
CT–CT–HC	109.95	341.2	110.7	156.9
CO–CT–HC	109.02	323.9	110.7	156.9
CT–CO–HC	111.41	340.3	110.7	156.9
CT–CT–OH	110.87	480.2	109.5	209.2
CO–CT–OH	110.62	515.2	109.5	209.2
CT–CT–OSB	109.24	370.5	109.5	209.2
CT–CT–OSR	109.24	444.0	109.5	209.2
CT–CO–OSB	110.40	413.3	109.5	209.2
CT–CO–OSR	110.40	458.6	109.5	209.2
CT–CO–OH	114.22	506.3	109.5	209.2
CT–OSB–CO	108.12	320.9	109.5	251.0
CT–OSR–CO	108.10	307.7	109.5	251.0
CT–OH–HO	110.10	373.4	108.5	230.1
CO–OH–HO	113.67	364.8	108.5	230.1
HC–CT–HC	108.21	331.1	107.8	138.1
HC–CT–OSB	108.01	402.0	109.5	146.4
HC–CT–OSR	108.04	410.5	109.5	146.4
HC–CT–OH	109.84	365.0	109.5	146.4
HC–CO–OSB	108.60	312.9	109.5	146.4
HC–CO–OSR	108.63	378.8	109.5	146.4
HC–CO–OH	112.80	377.0	109.5	146.4
OSB–CO–OSR	108.80	589.5	111.6	387.4
OSR–CO–OH	106.75	731.5	111.6	387.4

Table S–5: Optimized torsional coefficients V_n for cellulose in comparison to the literature force field of W. Damm *et al.*[7]

Torsion Angle	BILFF				Literature[7]			
	V_1 kJ mol^{-1}	V_2 kJ mol^{-1}	V_3 kJ mol^{-1}	V_4 kJ mol^{-1}	V_1 kJ mol^{-1}	V_2 kJ mol^{-1}	V_3 kJ mol^{-1}	V_4 kJ mol^{-1}
HC–CT–CT–HC	0.0000	0.0000	1.3305	0.0000	0.0000	0.0000	1.3305	0.0000
HC–CO–CT–HC	0.0000	0.0000	1.3305	0.0000	0.0000	0.0000	1.3305	0.0000
HC–CT–CT–CT	0.0000	0.0000	1.5313	0.0000	0.0000	0.0000	1.5313	0.0000
HC–CO–CT–CT	0.0000	0.0000	1.5313	0.0000	0.0000	0.0000	1.5313	0.0000
HC–CT–CT–CO	0.0000	0.0000	1.5313	0.0000	0.0000	0.0000	1.5313	0.0000
CT–CT–CT–CT	7.2802	−0.6569	1.1673	0.0000	7.2802	−0.6569	1.1673	0.0000
CT–CT–CT–CO	7.2802	−0.6569	1.1673	0.0000	7.2802	−0.6569	1.1673	0.0000
HC–CT–CT–OH	0.0000	0.0000	1.9581	0.0000	0.0000	0.0000	1.9581	0.0000
HC–CT–CT–OSB	0.0000	0.0000	1.9581	0.0000	0.0000	0.0000	1.9581	0.0000
HC–CT–CT–OSR	0.0000	0.0000	1.9581	0.0000	0.0000	0.0000	1.9581	0.0000
HC–CT–CO–OSB	0.0000	0.0000	1.9581	0.0000	0.0000	0.0000	1.9581	0.0000
HC–CT–CO–OSR	0.0000	0.0000	1.9581	0.0000	0.0000	0.0000	1.9581	0.0000
HC–CO–CT–OH	0.0000	0.0000	1.9581	0.0000	0.0000	0.0000	1.9581	0.0000
HC–CT–CO–OH	0.0000	0.0000	1.9581	0.0000	0.0000	0.0000	1.9581	0.0000
HC–CT–OH–HO	0.0000	0.0000	1.8828	0.0000	0.0000	0.0000	1.8828	0.0000
HC–CO–OH–HO	0.0000	0.0000	1.8828	0.0000	0.0000	0.0000	1.8828	0.0000
HC–CT–OSB–CO	0.0000	0.0000	3.1798	0.0000	0.0000	0.0000	3.1798	0.0000
HC–CT–OSR–CO	0.0000	0.0000	3.1798	0.0000	0.0000	0.0000	3.1798	0.0000
HC–CO–OSB–CT	0.0000	0.0000	3.1798	0.0000	0.0000	0.0000	3.1798	0.0000
HC–CO–OSR–CT	0.0000	0.0000	3.1798	0.0000	0.0000	0.0000	3.1798	0.0000
CO–OSB–CT–CT	2.7196	−1.0460	2.8033	−4.1840	2.7196	−1.0460	2.8033	0.0000
CO–OSR–CT–CT	2.7196	−1.0460	2.8033	−4.1840	2.7196	−1.0460	2.8033	0.0000
CT–OSB–CO–CT	2.7196	−8.3680	8.3680	0.0000	2.7196	−1.0460	2.8033	0.0000
CT–OSR–CO–CT	2.7196	−8.3680	8.3680	0.0000	2.7196	−1.0460	2.8033	0.0000
CT–OSB–CO–OSR	−1.5690	−5.6819	4.1840	0.0000	−1.5690	−5.6819	0.0167	0.0000
CT–OSR–CO–OSB	−1.5690	−5.6819	4.1840	0.0000	−1.5690	−5.6819	0.0167	0.0000
CT–OSR–CO–OH	−1.5690	−5.6819	0.0167	0.0000	−1.5690	−5.6819	0.0167	0.0000
OSR–CO–OH–HO	−5.2593	−7.5563	0.0126	0.0000	−5.2593	−7.5563	0.0126	0.0000
CT–CT–CT–OH	−5.5898	0.0000	0.0000	0.0000	−5.5898	0.0000	0.0000	0.0000
CT–CT–CT–OSB	−5.5898	0.0000	0.0000	0.0000	−5.5898	0.0000	0.0000	0.0000
CT–CT–CT–OSR	−5.5898	0.0000	0.0000	0.0000	−5.5898	0.0000	0.0000	0.0000
CT–CT–CO–OSB	−5.5898	0.0000	0.0000	0.0000	−5.5898	0.0000	0.0000	0.0000
CT–CT–CO–OSR	−5.5898	0.0000	0.0000	0.0000	−5.5898	0.0000	0.0000	0.0000
CT–CT–CO–OH	−5.5898	0.0000	0.0000	0.0000	−5.5898	0.0000	0.0000	0.0000
CO–CT–CT–OH	−5.5898	0.0000	0.0000	0.0000	−5.5898	0.0000	0.0000	0.0000
CT–CT–OH–HO	11.1880	−12.0625	4.2928	0.0000	11.1880	−12.0625	4.2928	0.0000
CO–CT–OH–HO	11.1880	−12.0625	4.2928	0.0000	11.1880	−12.0625	4.2928	0.0000
CT–CO–OH–HO	11.1880	−12.0625	4.2928	0.0000	11.1880	−12.0625	4.2928	0.0000
OH–C –C –OS	18.0707	0.0000	0.0000	0.0000	11.1880	−12.0625	4.2928	0.0000
OH–CT–CT–OSB	18.0707	0.0000	0.0000	0.0000	18.0707	0.0000	0.0000	0.0000
OH–CT–CT–OSR	18.0707	0.0000	0.0000	0.0000	18.0707	0.0000	0.0000	0.0000
OSR–CT–CT–OSB	18.0707	0.0000	0.0000	0.0000	18.0707	0.0000	0.0000	0.0000
OH–CT–CO–OSB	18.0707	0.0000	0.0000	0.0000	18.0707	0.0000	0.0000	0.0000
OH–CT–CO–OSR	18.0707	0.0000	0.0000	0.0000	18.0707	0.0000	0.0000	0.0000
OH–CT–CT–OH	37.9321	0.0000	0.0000	0.0000	37.9321	0.0000	0.0000	0.0000
OH–CO–CT–OH	37.9321	0.0000	0.0000	0.0000	37.9321	0.0000	0.0000	0.0000

2 Distribution Functions

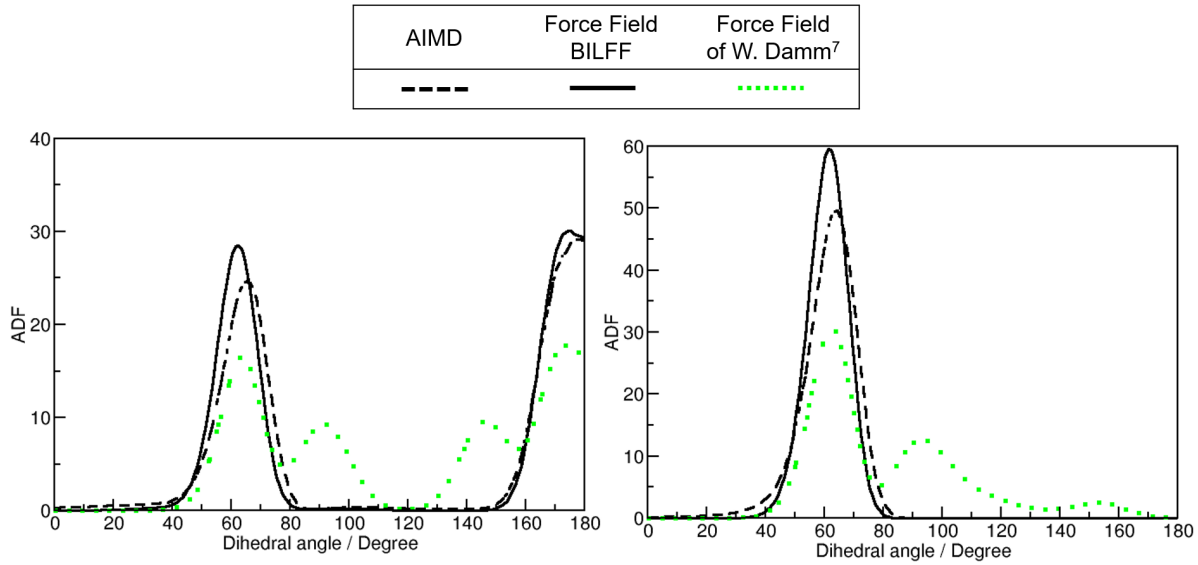

Figure S–2: Comparison of the angular distribution function of the dihedral angles CO–OSR–CT–CT *(left)* and CT–CO–OSR–CT *(right)* from the reference AIMD and the force field MD simulation using BILFF and the literature force field.[7]

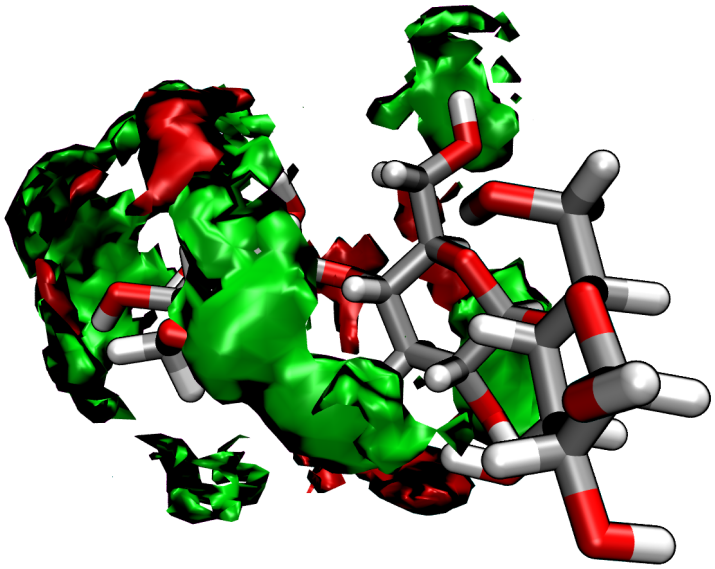

Figure S–3: Spatial distribution function of the ring protons of $[EMIm]^+$ (red, $13\,nm^{-3}$) and the acetate oxygen (green, $14\,nm^{-3}$) averaged over all glucose units in the cellulose–IL system in the reference AIMD simulation.

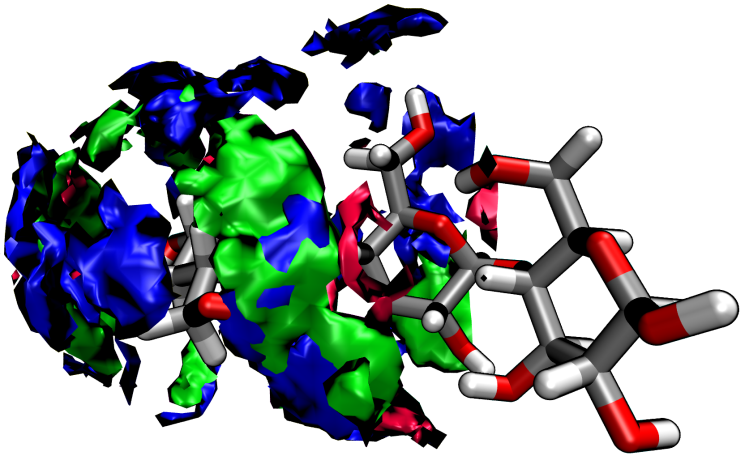

Figure S–4: Spatial distribution function of the ring protons of $[EMIm]^+$ (red, $9\,nm^{-3}$), acetate (green, $19\,nm^{-3}$) and water (blue, $25\,nm^{-3}$) averaged over all glucose units in the cellulose–IL–water system in the reference AIMD simulation.

3 Investigation of the Statistical Variance of the Radial Distribution Function

In this section, the radial distribution functions of the hydrogen bonds between the hydroxyl protons of cellulose of type HO6 *(see Fig. S–5)* and HOR *(see Fig. S–6)* and the oxygen atoms of acetate are shown. As already described in the main text, the individual RDFs of the observed atoms were averaged and weighted according to their position in the molecule *(see Section 3 in the main text)*. The results were obtained from eleven force field MD simulations using our new parameters of the pure cellulose–[EMIm][OAc] system. Each of the simulations were performed with a different randomly generated velocity initialization but with the same force field parameters. All other simulation parameters are identical to each other. By differentiating the velocity initialization, a statistical variance of the results could be produced, which serve to evaluate our RDFs shown in the main text (here colored in black). This therefore represents a benchmark for the ergodicity of the simulations. As expected, a diversity of the height of the first maxima becomes observable. The position of those maxima is identical. This proves that the results of the force field simulations shown in the main text are within the variation range.

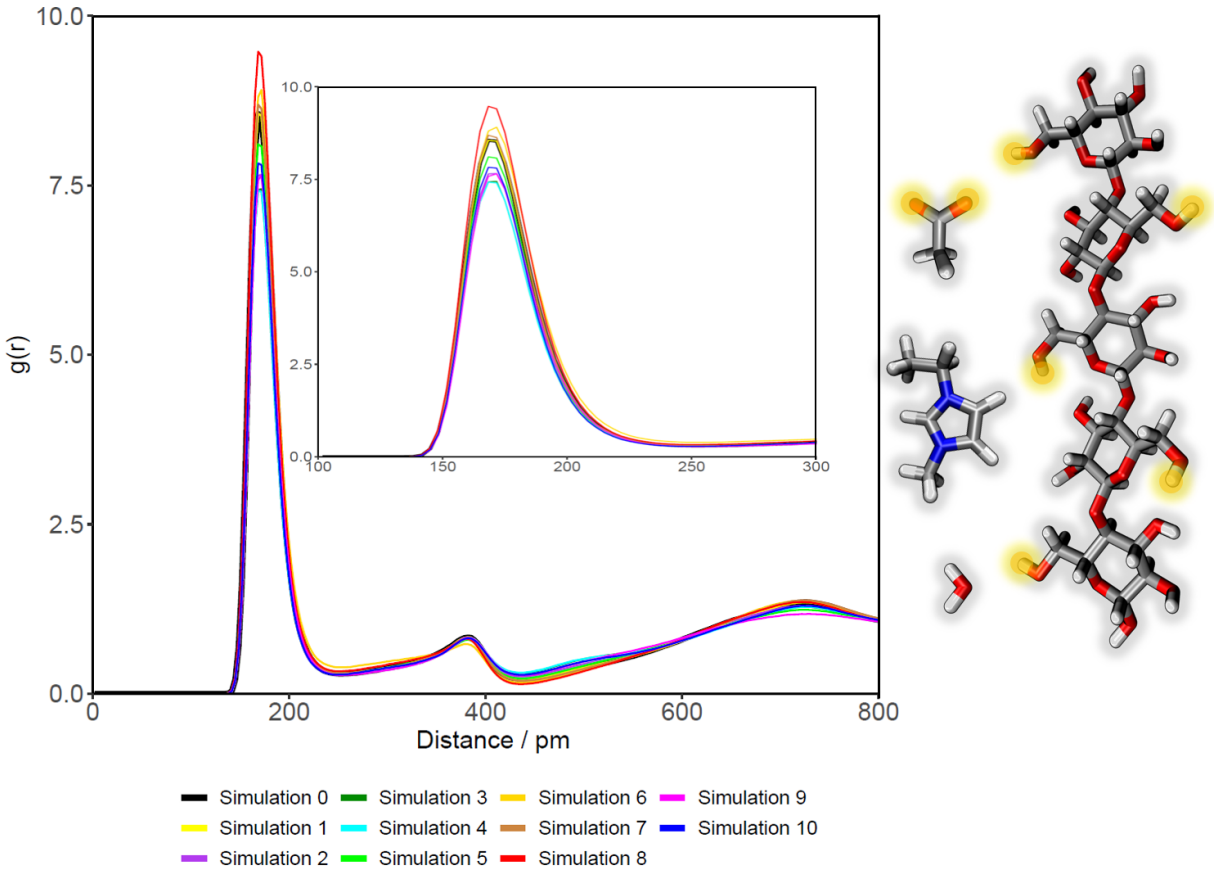

Figure S–5: Radial distribution functions of HO6-type hydroxyl protons from cellulose to acetate oxygen atoms in the pure cellulose–[EMIm][OAc] system. The force field simulations were performed with randomly generated different velocity initializations but with the same force field parameters of BILFF.

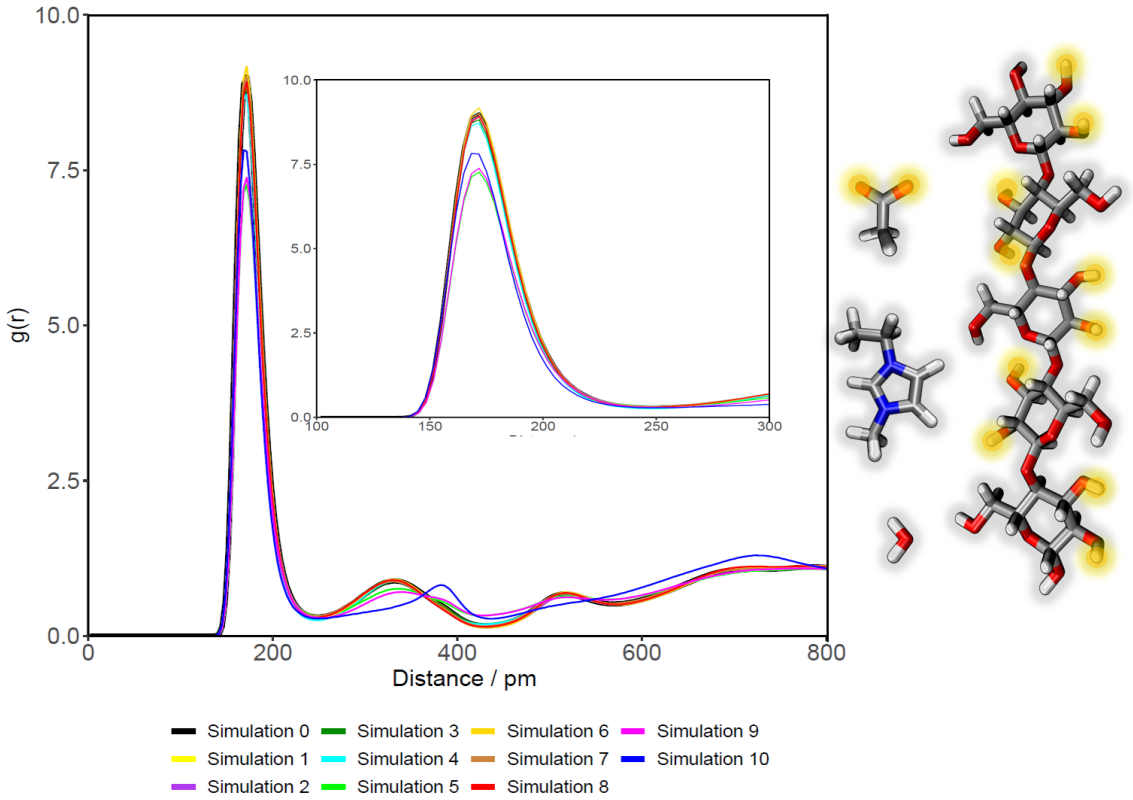

Figure S–6: Radial distribution functions of HOR-type hydroxyl protons from cellulose to acetate oxygen atoms in the pure cellulose–[EMIm][OAc] system. The force field simulations using BILFF were performed with randomly generated different velocity initializations.

4 Contact Matrices

In this section, the contact matrices from the AIMD simulations of the pure and aqueous cellulose–[EMIm][OAc] systems are shown. The numbering of the protons and oxygen atoms of cellulose used in the contact matrices calculated from the AIMDs is shown in Figure S–7. Figure S–8 presents the numbering of the cellulose atoms in the force field MD simulations.

In both cellulose–IL systems, hydrogen bonds between the hydroxyl protons of cellulose and the oxygen atoms of acetate and water are dominant, as well as hydrogen bonds between the protons of water and the oxygen atoms of cellulose. Hydrogen bonds are also formed between the ring protons of $[EMIm]^+$ and the oxygen atoms of cellulose. The AIMD simulations thus show the same trends of the hydrogen bond network as the force field simulations with BILFF.

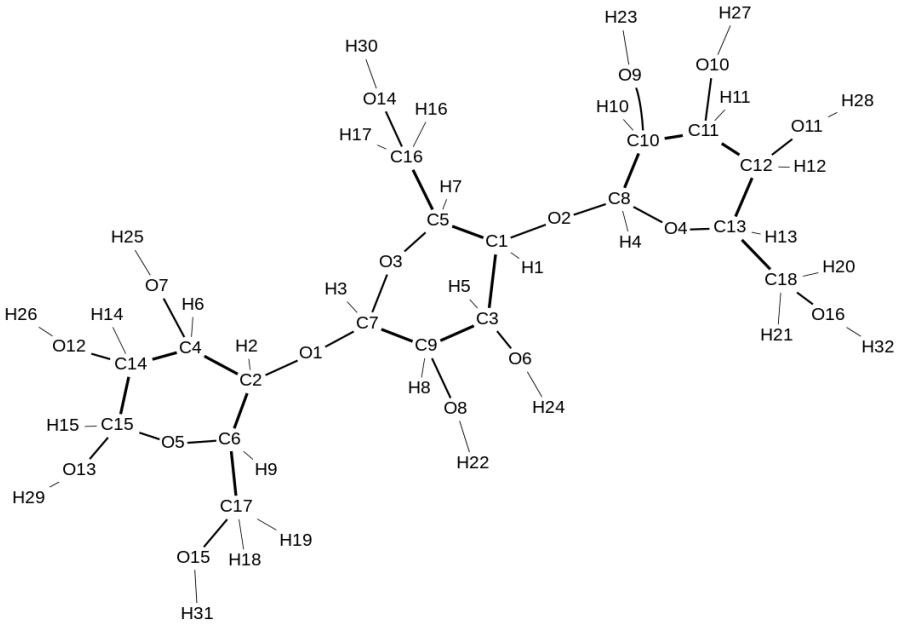

Figure S–7: Numbering of the protons and oxygen atoms of cellulose used in the contact matrices calculated from the AIMD simulations.

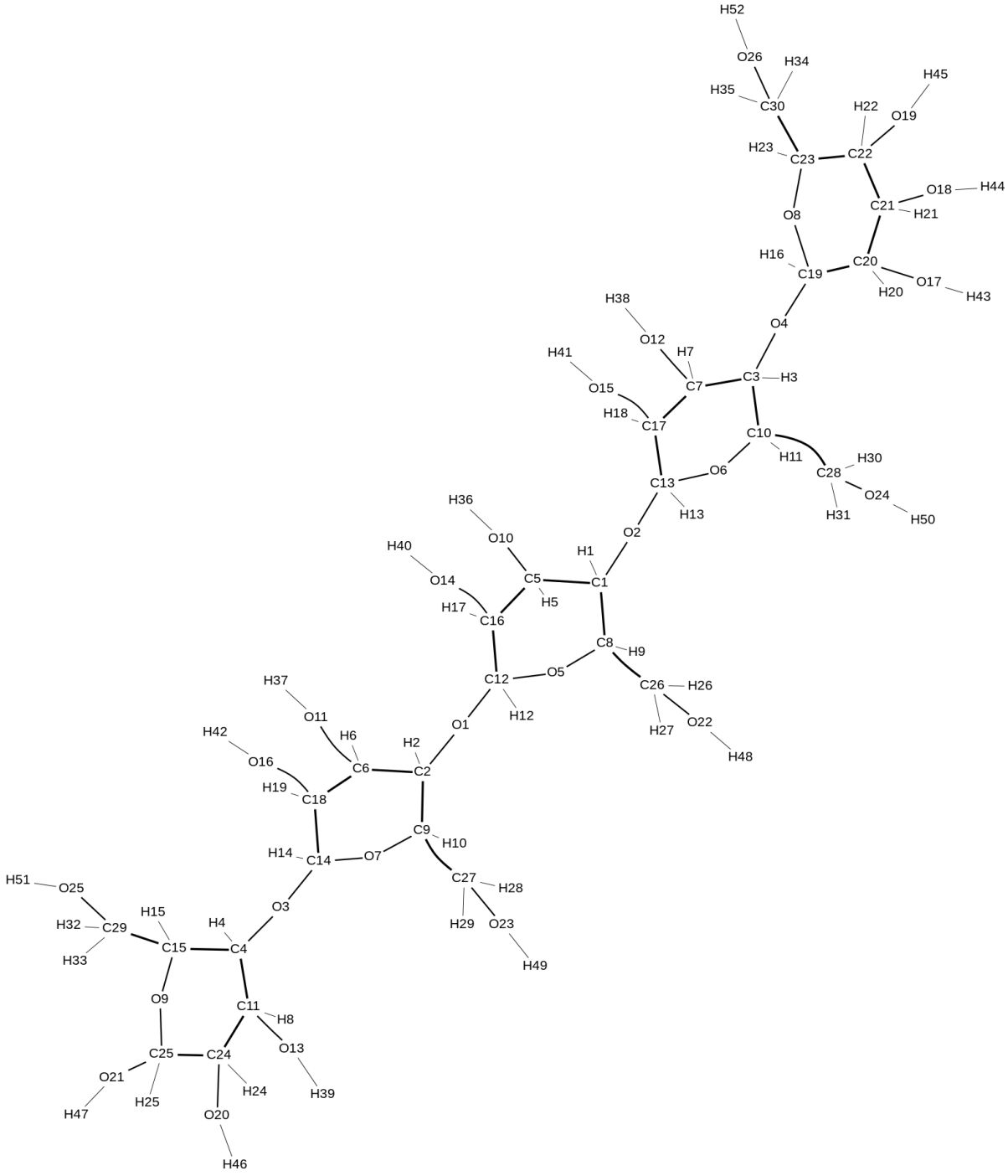

Figure S–8: Numbering of the protons and oxygen atoms of cellulose used in the contact matrices calculated from the force field MD simulations.

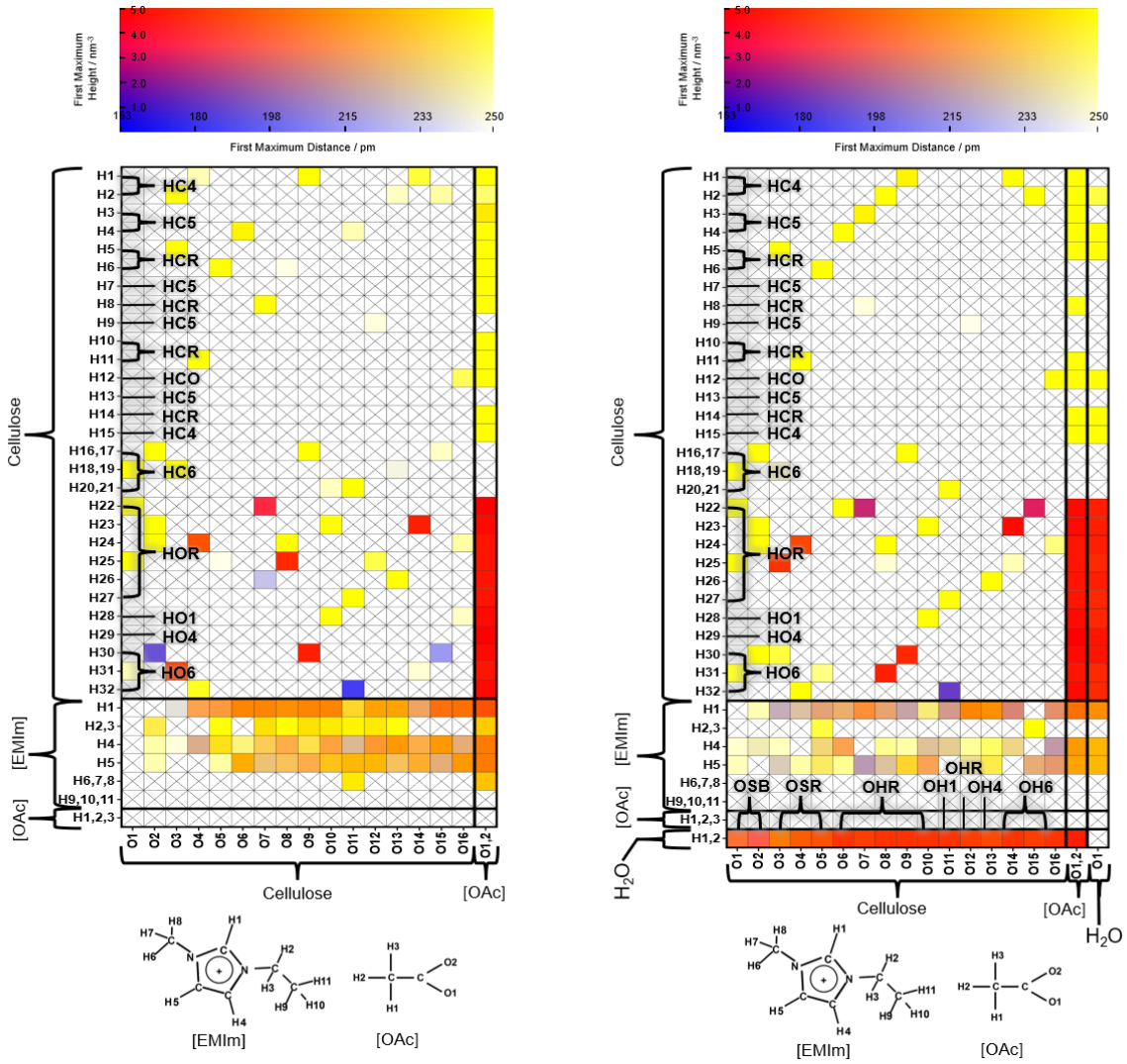

Figure S–9: Contact matrix illustrating hydrogen bonding in the cellulose–[EMIm][OAc] system in absence *(left)* and presence *(right)* of water from the reference AIMD simulation. For a better understanding, the atom types of cellulose are noted in the matrix and the atom numbers of the relevant atoms of the ionic liquid are shown below.

References

(1) Jorgensen, W. L.; Maxwell, D. S.; Tirado-Rives, J. Development and Testing of the OPLS All-Atom Force Field on Conformational Energetics and Properties of Organic Liquids. J. Am. Chem. Soc. **1996**, 118, 11225–11236.

(2) Ponder, J. W.; Case, D. A. Force Fields for Protein Simulations. Adv. Protein Chem. **2003**, 66, 27–85.

(3) Sambasivarao, S. V.; Acevedo, O. Development of OPLS-AA Force Field Parameters for 68 Unique Ionic Liquids. J. Chem. Theory Comput. **2009**, 5, 1038–1050.

(4) Plimpton, S. Fast Parallel Algorithms for Short-Range Molecular Dynamics. J. Comp. Phys. **1995**, 117, 1–19.

(5) Roos, E.; Brehm, M. A force field for bio-polymers in ionic liquids (BILFF) - part 1: EMImOAc/water mixtures. Phys. Chem. Chem. Phys. **2021**, 23, 1242–1253.

(6) Horn, H. W.; Swope, W. C.; Pitera, J. W.; Madura, J. D.; Dick, T. J.; Hura, G. L.; Head-Gordon, T. Development of an improved four-site water model for biomolecular simulations: TIP4P-Ew. J. Chem. Phys **2004**, 120, 9665–9678.

(7) Damm, W.; Frontera, A.; Tirado-Rives, J.; Jorgensen, W. L. OPLS all-atom force field for carbohydrates. J. Comput. Chem. **1997**, 18, 1955–1970.